A Quadruple-Polarization Reconfigurable Feeding Network for UAV RF Sensing Antenna

Dong-Geun Seo, Ji-Hong Kim, Manos M. Tentzeris, *Fellow, IEEE*, and Wang-Sang Lee, *Member, IEEE*

***Abstract*— A quadruple-polarization reconfigurable feeding network for an unmanned aerial vehicle (UAV) RF sensing antenna operating at 915 MHz is presented. It consists of one single-pole four-throw (SP4T) switch, one 90° hybrid coupler, two 180° hybrid couplers, and two single-pole double-throw (SPDT) switches. By controlling the SP4T and SPDT switches, quadruple polarizations with two linear polarizations (vertical and horizontal) and two circular polarizations (right-hand and left-hand) were obtained. The proposed reconfigurable feeding network with quadruple polarization modes in the 902–928-MHz range has an insertion loss of approximately 2.5 dB including switch loss, and it achieves amplitude and phase variations of up to approximately 0.5 dB without divided power or switch loss, and 3°, respectively. Using the proposed feeding network, a circular low-profile UAV RF sensing antenna with quadruple polarizations was designed. Its electrical size, 10-dB impedance bandwidths, and a peak gain are approximately $0.57\lambda_0 \times 0.57\lambda_0 \times 0.08\lambda_0$ at 915 MHz, 16%, and 6 dBi(c), respectively.**

***Index Terms*— Quadruple-polarization, reconfigurable feeding network, RF sensing, UAV antenna.**

I. Introduction

In RECENT years, unmanned aerial vehicles (UAV) have been studied for a wide range of applications. It is possible to solve many problems using remote control. In industry, drones with radio frequency identification can be used for efficient inventory management and equipment maintenance. In military applications, UAVs are used as surveillance vehicles and to perform missions in extreme situations. For these tasks, it is essential to apply an antenna with high efficiency, high gain, and large beam coverage. In addition, for wireless communication, the polarization mode is also an important factor. If a receiver has a fixed polarization, the transmitter should match it to reduce polarization loss because such loss severely degrades data communication performance. To address these issues, many studies have been conducted [1]–[12]. In [1]–[5], dipole antennas were used with p-i-n diodes. To obtain a wide bandwidth, a crossed dipole antenna was presented in [1] and [2]. Ge *et al*. [3] proposed the multipolarization by switching between a patch shape and a stripline in a magnetoelectric dipole antenna. In another study by Hu *et al*. [6], metasurfaces were used to form periodic square patch elements. Liu *et al*. [7] proposed using a simply printed monopole to control frequency and polarization. Studies using patch antennas have also been carried out [8]–[11]. Lee *et al*. [8] proposed a reconfigurable antenna using a T-shaped feed. In this design, switching between linear polarization (LP) and circular polarization (CP) is achieved through two p-i-n diodes and two conductive pads connected to the ground through a via hole. Nguyen-Trong *et al*. [9] added varactors on a patch antenna. Slot-based switching polarization mode has also been proposed [10], [11]. However, in these previous papers, the p-i-n diodes directly connected to an antenna can affect its performance such as antenna radiation efficiency deterioration due to their losses within practical systems. Also, it is difficult to integrate these designs into a system due to their complicated topologies. Therefore, we present a quadruple-polarization feeding reconfigurable network for an RF sensing antenna. In our previous work [12], we proposed a quadruple-polarized reconfigurable antenna using one 90° hybrid coupler and one single-pole four-throw (SP4T) switch. To address this problem, we propose an improved quadruple-polarization method that is superior to the conventional ones. In this letter, we propose as a proof-of-concept the demonstration an improved quadruple-polarization reconfigurable feeding network and a UAV RF sensing antenna using the quadruple selective control for operation in the 915-MHz industry, science, and medical (ISM) band.

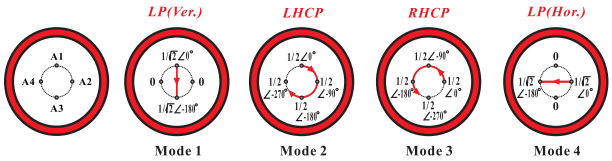

Fig. 1. Front view of the feeding points of the proposed antenna and each polarization mode operation.

II. Polarization-Reconfigurable Feeding Network and UAV Antenna Topology

Fig. 1 depicts the four modes of polarization achieved with the proposed topology. The feeding network comprises four-port feeding microstrip lines, one 90° hybrid coupler,

Manuscript received December 31, 2018; accepted January 31, 2019. Date of publication February 20, 2019; date of current version March 11, 2019. This work was supported in part by the Ministry of Science and ICT (MSIT), South Korea, through the Institute for Information and Communications Technology Promotion (IITP)–A study on a small antenna system for vehicle supporting wide elevation angle–under Grant 2017-0-00795 and in part by the Ministry of Trade, Industry and Energy (MOTIE), South Korea, through the Human Resources Program in Energy Technology of the Korea Institute of Energy Technology Evaluation and Planning (KETEP) under Grant 20174030201440. *(Corresponding author: Wang-Sang Lee.)*

D.-G. Seo and W.-S. Lee are with the Department of Electronic Engineering, Engineering Research Institute, Gyeongsang National University, Jinju 52828, South Korea (e-mail: wsang@gnu.ac.kr).

J.-H. Kim was with Gyeongsang National University, Jinju 52828, South Korea. He is now with the Aeronautical Systems Team 1, Defense Agency for Technology and Quality (DTaQ), Jinju 52851, South Korea.

M. M. Tentzeris is with the School of Electrical and Computer Engineering, Georgia Institute of Technology, Atlanta, GA 30332 USA.

Color versions of one or more of the figures in this paper are available online at http://ieeexplore.ieee.org.

Digital Object Identifier 10.1109/LMWC.2019.2897479

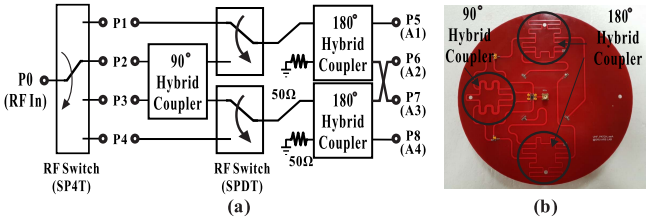

Fig. 2. Proposed feeding network. (a) Overall block diagram and (b) its implementation.

TABLE I

OPERATING POLARIZATION MODES OF THE PROPOSED RECONFIGURABLE FEEDING NETWORK

Distributions (Ampli., Phase)		Input			
		P1	P2	P3	P4
Output	P5 (A1)	$\frac{1}{\sqrt{2}}$, 0°	$\frac{1}{2}$, 0°	$\frac{1}{2}$, -90°	0, NA
	P6 (A2)	0, NA	$\frac{1}{2}$, -90°	$\frac{1}{2}$, 0°	$\frac{1}{\sqrt{2}}$, 0°
	P7 (A3)	$\frac{1}{\sqrt{2}}$, -180°	$\frac{1}{2}$, -180°	$\frac{1}{2}$, -270°	0, NA
	P8 (A4)	0, NA	$\frac{1}{2}$, -270°	$\frac{1}{2}$, -180°	$\frac{1}{\sqrt{2}}$, -180°
SPDT States		P1, NA	P2, P3	P2, P3	NA, P4
Polar. Modes		V-LP	LHCP	RHCP	H-LP

two 180° hybrid couplers, one SP4T, and two single-pole double-throw (SPDT) switches. Using the feeding network, LP and CP are obtained by controlling the RF switches appropriately. Fig. 2 shows the proposed feeding network. Its polarization mode is selected by using the SP4T switch when the RF input signal is applied. The LP mode is realized by selecting P1 and P4, while the CP mode is realized by selecting P2 and P3. When P1 is selected, output ports A1 and A3 are operated with 180° phase difference by passing through the 180° hybrid coupler, thus a vertical LP (V-LP) is realized. A horizontal LP (H-LP) that is orthogonal with regard to the V-LP is realized when the P4 is selected. On the other hand, the left-hand CP (LHCP) mode is made up of selecting P2. This signal splits in two half-power paths due to the 90° hybrid coupler. Then, when the top SPDT switch selects P2, the four output paths feature 90° progressive phase variation due to the use of the two 180° hybrid couplers dividing half power signal. As a result, the mode output of the feeding network is summarized in Table I. The input switches of the four polarization modes are denoted by P1–P4. The output ports of the feeding network are denoted by P5(A1)–P8(A4). The elements of the table are respectively the output power level and phase provided by the proposed feeding network.

Fig. 3(a) presents the proposed reconfigurable antenna configuration and its parameters, and Fig. 3(b) and (c) shows the fabricated feeding network and the antenna prototype. This antenna consists of two circular plates and two rectangular crossed supports using an FR-4 substrate. The radiator is positioned on the top layer of the upper metal plate. It has a metal plate on the bottom layer and a hole at its center to control the current flow. Therefore, the correct polarization mode and impedance matching are achieved. For wide impedance bandwidth, four-port tapered feed lines on one side of the crossed rectangular support using two 0.8-mm-thick FR-4 substrates are printed as shown in Fig. 3(c). To integrate a feeding network while enhancing the antenna gain, a metallic reflector with clearances between the ground plane and the

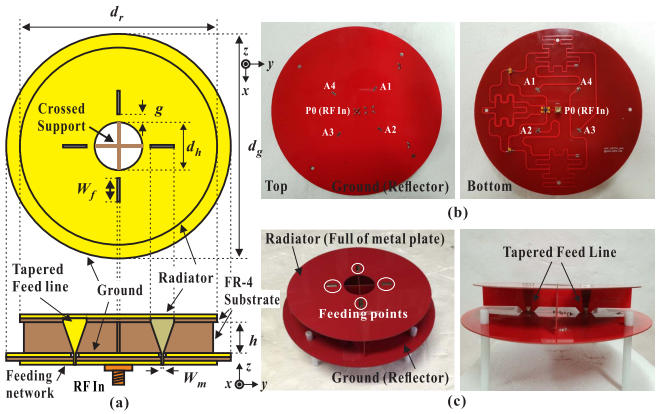

Fig. 3. Proposed antenna configuration. (a) Front and side views. (b) Fabricated feeding network. (c) Antenna prototype.

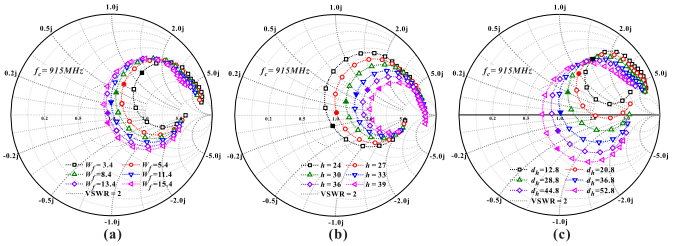

Fig. 4. Simulated input impedance variations of the proposed antenna. (a) Feed slot width (W_f). (b) Antenna height (h). (c) Hole diameter (d_h). The occupied symbol means the center frequency (f_c, 915 MHz).

feed lines is added to the top layer of the bottom substrate while being used simultaneously as the ground plane for the microstrip lines of the feeding. Finally, for the miniaturized design, the proposed feeding network using the meandered line structure is printed on the bottom layer of the lower plate. Fig. 4 indicates the impedance variation characteristics of the proposed antenna. According to the parameter sweep of feed slot width (W_f), antenna height (h), and hole diameter (d_h), the optimized values are obtained for impedance matching. The implemented parameters shown in Fig. 3(a) are $d_r = 166$ mm, $d_g = 188$ mm, $g = 7.5$ mm, $d_h = 36.8$ mm, $W_f = 13.4$ mm, $h = 27$ mm, and $W_m = 4.1$ mm.

III. RESULT AND DISCUSSION

The proposed UAV antenna with the proposed feeding network operated in the 915-MHz ISM band has been optimized using CST Microwave Studio 2018. To miniaturize the antenna design, the proposed antenna was fabricated on an FR-4 substrate of 0.8 mm thickness and a copper thickness of 18 um. The SP4T and SPDT switches for selecting and making each polarization mode were SKY13322-375LF and AS179-92LF made by Skyworks, respectively. The measured results of the feeding network are presented in Fig. 5. The reflection coefficients for quadruple-polarization modes shown in Fig. 5(a) were less than -10 dB, which include the insertion losses of an SPDT switch and hybrid couplers. In the case of dual orthogonal LP shown in Fig. 5(b), the phase variation is approximately 180°, and the transmission coefficient including 3 dB divided power loss is approximately -5.2 dB at 915 MHz. On the other hand, the phase variation of CP

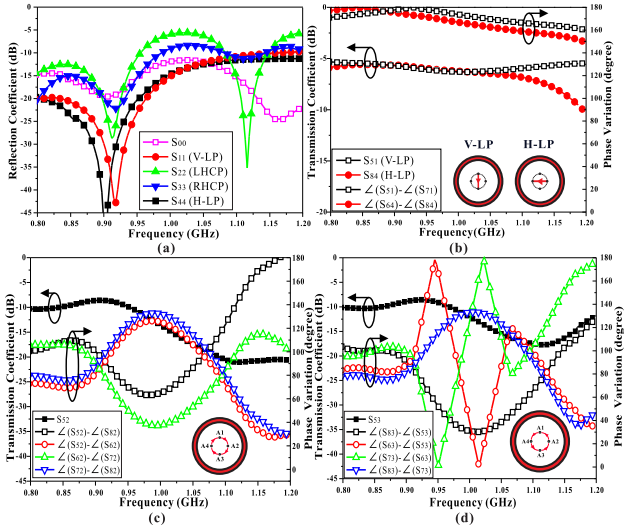

Fig. 5. Measured results of the proposed feeding network. (a) Reflection coefficient of LPs. (b) Transmission coefficient and phase variation of V-LP and H-LP. (c) Transmission coefficient and phase variation of LHCP. (d) Transmission coefficient and phase variation of RHCP.

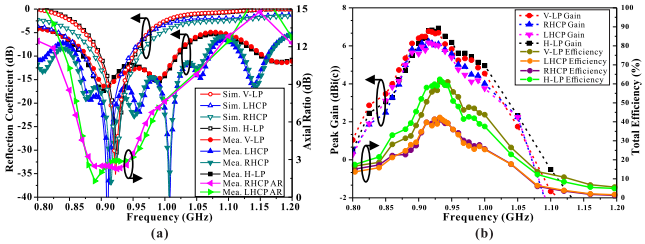

Fig. 6. Characteristic of the proposed antenna at each polarization mode. (a) Simulated and measured reflection coefficients as well as ARs. (b) Measured peak gains and total efficiencies.

mode is approximately 90° as shown in Fig. 5(c)–(d), and the transmission coefficient including 6 dB divided power loss is approximately −8.5 dB. Fig. 6(a) depicts the simulated and measured reflection coefficients as well as axial ratios (ARs) for the proposed antenna. The 10-dB impedance bandwidths of LP and CP modes are approximately 15.85% from 875 MHz to 1.02 GHz and 18% from 860 MHz to 1.025 GHz, respectively. Moreover, the 3-dB AR bandwidths of CP modes cover approximately 7.1% from 880 to 945 MHz. Since the phase differences at CP modes formed through 90° and 180° hybrid couplers shown in Fig. 2(a) are increased, the AR bandwidth has become narrower. Fig. 6(b) shows the peak gain and total efficiency with regard to the operating frequency. The peak gains are more than 6 dBi(c) at each mode, and the total efficiencies of LP and CP modes are approximately 60% and 40%, respectively. In Fig. 7, the elevation radiation patterns (xz plane) are compared to simulated and measured results at each mode. The measured cross polarizations are less than approximately −20 dB at two LP modes and approximately −10 dB at two CP modes. The half-power beamwidth is approximately 60°. Table II describes the performance comparisons with other state-of-the-art multiple-polarized antennas. Therefore, the proposed antenna with the quadruple-polarization reconfigurable feeding network could be useful for UAV applications due to a low-profile balanced antenna structure as well as ease of multiple polarization control.

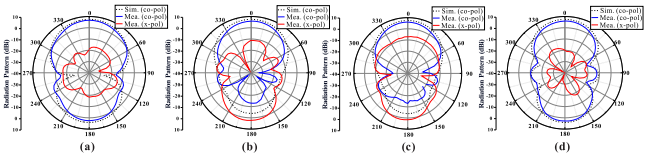

Fig. 7. Simulated and measured radiation patterns in the xz plane at 915 MHz. (a) V-LP. (b) LHCP. (c) RHCP. and (d) H-LP.

TABLE II
PERFORMANCE COMPARISONS OF MULTIPLE POLARIZED ANTENNAS

Ref.	f_c (GHz)	BW, Gain (%, dBi(c))	Polar. (EA)	AR (%)	Elect. Size (λ_0^3)
[4]	1.67	80, 4.8	2	23.5	0.84×0.84×0.28
[6]	5.6	16, 9.4	4	16	1.30×1.30×0.07
[10]	2.45	7, 5.3	4	-	0.57×0.57×0.07
[11]	2.45	1.2, 5.8	3	0.8	0.65×0.65×0.01
[12]	0.915	5.8, 6	4	1	0.53×0.53×0.08
Prop.	**0.915**	**16, 6**	**4**	**7**	**0.57×0.57×0.08**

IV. CONCLUSION

A 915-MHz quadruple-polarization reconfigurable feeding network for a UAV RF sensing antenna was presented. By electrically switching the quadruple modes such as V-LP, H-LP, LHCP, and RHCP, the proposed antenna can reduce the polarization loss. In addition, because the proposed antenna has a low-profile balanced structure as well as ease of multiple polarization control, it is useful for performing missions using UAVs in many fields.

REFERENCES

[1] J.-S. Row and Y.-H. Wei, "Wideband reconfigurable crossed-dipole antenna with quad-polarization diversity," *IEEE Trans. Antennas Propag.*, vol. 66, no. 4, pp. 2090–2094, Apr. 2018.

[2] H. H. Tran, N. Nguyen-Trong, T. T. Le, and H. C. Park, "Wideband and multipolarization reconfigurable crossed bowtie dipole antenna," *IEEE Trans. Antennas Propag.*, vol. 65, no. 12, pp. 6968–6975, Dec. 2017.

[3] L. Ge, X. Yang, M. Li, and H. Wong, "Polarization-reconfigurable magnetoelectric dipole antenna for 5G Wi-Fi," *IEEE Antennas Wireless Propag. Lett.*, vol. 16, pp. 1504–1507, 2017.

[4] W. Lin and H. Wong, "Wideband circular polarization reconfigurable antenna," *IEEE Trans. Antenna Propag.*, vol. 63, no. 12, pp. 5938–5944, Dec. 2015.

[5] H. Wong, W. Lin, L. Huitema, and E. Arnaud, "Multi-polarization reconfigurable antenna for wireless biomedical system," *IEEE Trans. Biomed. Circuits Syst.*, vol. 11, no. 3, pp. 652–660, Jun. 2017.

[6] J. Hu, G. Q. Luo, and Z.-C. Hao, "A wideband quad-polarization reconfigurable metasurface antenna," *IEEE Access*, vol. 6, pp. 6130–6137, 2018.

[7] J. Liu, J. Li, and R. Xu, "Design of very simple frequency and polarisation reconfigurable antenna with finite ground structure," *Electron. Lett.*, vol. 54, no. 4, pp. 187–188, Feb. 2018.

[8] S. W. Lee and Y. J. Sung, "Simple polarization-reconfigurable antenna with T-shaped feed," *IEEE Antennas Wireless Propag. Lett.*, vol. 15, pp. 114–117, 2016.

[9] N. Nguyen-Trong, L. Hall, and C. Fumeaux, "A frequency- and polarization-reconfigurable stub-Loaded microstrip patch antenna," *IEEE Trans. Antennas Propag.*, vol. 63, no. 11, pp. 5235–5240, Nov. 2015.

[10] S.-L. Chen, F. Wei, P.-Y. Qin, Y. J. Guo, and X. Chen, "A multi-linear polarization reconfigurable unidirectional patch antenna," *IEEE Trans. Antennas Propag.*, vol. 65, no. 8, pp. 4299–4304, Aug. 2017.

[11] X.-X. Yang, B.-C. Shao, F. Yang, A. Z. Elsherbeni, and B. Gong, "A polarization reconfigurable patch antenna with loop slots on the ground plane," *IEEE Antennas Wireless Propag. Lett.*, vol. 11, pp. 69–72, 2012.

[12] J.-H. Kim, C.-H. Joo, S.-H. Ahn, and W.-S. Lee, "A quadruple-polarized reconfigurable antenna for 915 MHz ISM band applications," in *Proc. IEEE Int. Conf. Consum. Electron. (ICCE)*, Las Vegas, NV, USA, Jan. 2018, pp. 1–2.